



3 1176 00095 4298

10  
Copy 2  
**NATIONAL ADVISORY COMMITTEE  
FOR AERONAUTICS**

**TECHNICAL NOTE**

No. 1423

**THE STABILITY DERIVATIVES OF LOW-ASPECT-RATIO TRIANGULAR  
WINGS AT SUBSONIC AND SUPERSONIC SPEEDS**

By Herbert S. Ribner

Langley Memorial Aeronautical Laboratory  
Langley Field, Va.

**FOR REFERENCE**

**NOT TO BE TAKEN FROM THIS ROOM**



Washington  
September 1947

**LIBRARY COPY**

APR 30 1993

LANGLEY RESEARCH CENTER  
LIBRARY NASA  
HAMPTON, VIRGINIA

E R R A T U M

NACA TN No. 1423

THE STABILITY DERIVATIVES OF LOW-ASPECT-RATIO TRIANGULAR  
WINGS AT SUBSONIC AND SUPERSONIC SPEEDS

By Herbert S. Ribner  
September 1947

Page 32, table I: The fourth value listed under the column headed  
"Stability axes" should read

$$-\frac{1}{2}\pi A \frac{x_{cg}}{c}$$

NATIONAL ADVISORY COMMITTEE FOR AERONAUTICS

---

TECHNICAL NOTE NO. 1423

---

THE STABILITY DERIVATIVES OF LOW-ASPECT-RATIO TRIANGULAR  
WINGS AT SUBSONIC AND SUPERSONIC SPEEDS

By Herbert S. Ribner

S U M M A R Y

Low-aspect-ratio wings having triangular plan forms are treated on the assumption that the flow potentials in planes at right angles to the long axis of the airfoils are similar to the corresponding two-dimensional potentials. Pressure distributions caused by downward acceleration, pitching, rolling, sideslipping, and yawing are obtained for wings with and without dihedral. The stability derivatives calculated from these distributions are expected to apply at both subsonic and supersonic speeds, with the exception of the transonic region, up to a limiting speed at which the triangle is no longer narrow compared with the Mach cone from its vertex.

I N T R O D U C T I O N

The aerodynamics of slender symmetrical pointed airfoils moving point foremost may be approximated as Munk approximated the aerodynamics of slender airships (reference 1). For such bodies the flow is approximately two dimensional in planes perpendicular to the axis of symmetry. The assumption of two-dimensional flows leads to a very simple mathematical procedure for obtaining the pressure distribution. Reference 2 introduced this method and treated thereby the slender pointed airfoil at an angle of attack. The method is suited, as well, to the calculation of the pressure distributions due to normal acceleration, pitching, rolling, sideslipping, and yawing. In the present analysis the method in extended form is applied to the determination of these pressure distributions for a low-aspect-ratio triangular plan form. The stability derivatives of the airfoil are calculated from these results.

The analysis of the lifting airfoil showed that if the airfoil is very slender (very low aspect ratio) the results apply well into the supersonic range with no modification for the effect of compressibility. The transonic region probably must be excluded. The stability derivatives of this report are expected to have a similar range of application.

The principal part of this investigation was carried out during March and April of 1946.

### S Y M B O L S

V	flight velocity
x,y,z	rectangular coordinates (fig. 2)
u,v,w	incremental flight velocities along x-, y-, and z-axes of figure 1, respectively; induced flow velocities along x-, y-, and z-axes of figure 2, respectively
p,q,r	angular velocities about x-, y-, and z-axes, respectively (fig. 1)
u <sub>o</sub>	component of velocity induced on upper surface parallel to stream velocity
α	angle of attack
β	angle of sideslip
Γ	dihedral angle
ΔP	pressure difference between lower and upper surfaces of airfoil (positive in sense of lift)
ρ	density of air
a	semiwidth of triangle at distance x from vertex
b	span (base of triangle)
c	root chord (height of triangle)
$\bar{c}$	mean aerodynamic chord $\left( \bar{c} = \frac{2}{S} \int_0^{b/2} (\text{local chord})^2 dy = \frac{2c}{3} \right)$
A	aspect ratio $\left( \frac{2b}{c} \right)$

C	edge slope $\left(\frac{a}{x} = \frac{da}{dx} = \frac{A}{L}\right)$
S	area of triangle $\left(\frac{1}{2}bc\right)$
G	constant defined in equation (23)
$\phi$	surface velocity potential
$\eta$	$\cos^{-1} y/a$
L	rolling moment
L'	normal force (approximately lift)
M	pitching moment
N	yawing moment
Y	lateral force
F	suction force per unit length of edge
$C_L$	lift coefficient $\left(\frac{L'}{\frac{1}{2}\rho V^2 S}\right)$
$C_L$	rolling-moment coefficient $\left(\frac{L}{\frac{1}{2}\rho V^2 S b}\right)$
$C_m$	pitching-moment coefficient $\left(\frac{M}{\frac{1}{2}\rho V^2 S \bar{z}}\right)$
$C_n$	yawing-moment coefficient $\left(\frac{N}{\frac{1}{2}\rho V^2 S b}\right)$
$C_Y$	lateral-force coefficient $\left(\frac{Y}{\frac{1}{2}\rho V^2 S}\right)$
$C_{D_0}$	profile-drag coefficient $\left(\frac{\text{Profile drag}}{\frac{1}{2}\rho V^2 S}\right)$

$k$	vorticity
$A_0, A_1, \dots, A_m$	Fourier coefficients
$v_N$	induced surface velocity normal to wing leading edge
$s$	distance from wing leading edge measured normal to edge
$x_{cg}$	distance of center of gravity forward of $\frac{2}{3}c$

## Subscripts:

T.E.	at trailing edge
L.E.	at leading edge
R	at right leading edge
L	at left leading edge

## Subscripted parentheses:

$( )_\alpha$	contribution due to angle of attack
$( )_r$	contribution due to dihedral

Whenever  $\alpha$ ,  $\dot{\alpha}$ ,  $q$ ,  $p$ ,  $\beta$ , and  $r$  are used as subscripts, a nondimensional derivative is indicated and this derivative is the

slope through zero. For example,  $C_{m\dot{\alpha}} = \left[ \frac{\partial C_m}{\partial \left( \frac{\dot{\alpha}c}{2V} \right)} \right]_{\dot{\alpha}=0}$ ;  $C_{mq} = \left[ \frac{\partial C_m}{\partial \left( \frac{q\bar{c}}{2V} \right)} \right]_{q=0}$ ;

$$C_{lp} = \left[ \frac{\partial C_l}{\partial \left( \frac{pb}{2V} \right)} \right]_{p=0}; \quad C_{l\beta} = \left( \frac{\partial C_l}{\partial \beta} \right)_{\beta=0}; \quad C_{lr} = \left[ \frac{\partial C_l}{\partial \left( \frac{rb}{2V} \right)} \right]_{r=0}.$$

A dot above a symbol denotes differentiation with respect to time.

All angles are measured in radians.

## A N A L Y S I S

## SCOPE

The stability derivatives treated herein are listed, together with the values found for them, in table I. The derivations that follow give the values with reference to the principal body axes of figure 1 with origin at the aerodynamic center  $(\frac{2}{3}c, 0, 0)$ . Conversion has been made to the system of stability axes shown in figure 3 with origin a distance  $x_{cg}$  ahead of the  $\frac{2}{3}c$  point (transformation equations in reference 3). Table I comprises parallel columns which present the values relative to both systems.

## GENERAL

Consider a slender isosceles triangle moving with its vertex foremost along its longitudinal axis, as in figure 1, with velocity  $V$ . Small linear disturbance velocities  $u$ ,  $v$ , and  $w$  along the  $x$ -,  $y$ -, and  $z$ -axes and small angular disturbance velocities  $p$ ,  $q$ , and  $r$  about the  $x$ -,  $y$ -, and  $z$ -axes, respectively, may be contemplated. Angle of attack gives rise to  $w$ , sideslip, to  $v$ , and rolling, pitching, and yawing correspond to  $p$ ,  $q$ , and  $r$ , respectively.

As an example, suppose the sole disturbance velocity is  $w$ , caused by angle of attack. (This case forms the subject of reference 2.) The triangular airfoil is assumed to be moving forward with velocity  $V$  and downward with the small velocity  $\alpha V$ . The airfoil section is assumed to be very thin; therefore, only the downward motion disturbs the air. The triangular plan form is also assumed to be very slender so that the edges are nearly parallel. The flow in any plane  $x = \text{constant}$  (coordinate system of fig. 2) due to the downward motion is thus almost two dimensional. It may be expressed by the two-dimensional potential of a horizontal straight line moving downward with velocity  $\alpha V$ . The horizontal straight line is then the section of the airfoil cut by the plane  $x = \text{constant}$ . Planes  $x = \text{constant}$  may be taken anywhere from the apex to the trailing edge.

In case the disturbance velocity is rate of roll  $p$ , the straight line is to be regarded as rotating with angular velocity  $p$ . The other cases are somewhat more complicated and are discussed in detail in subsequent sections. In all cases, however, the initial problem is the determination of the two-dimensional surface potential for the flow about a straight line with assigned boundary conditions.

With the two-dimensional surface potential known for the motion of the section  $x = \text{constant}$ , the pressure difference between the upper and lower surfaces (positive upward) is obtained from

$$\Delta P = 2\rho V u_0 \quad (1)$$

In this equation  $u_0$  is the component of the velocity induced on the upper surface parallel to the stream direction and is obtained by differentiation of the potential in the stream direction. Equation (1) expresses Bernoulli's law with the approximation of small disturbances.

The assumption that the triangular plan form is very slender is expressed mathematically by the relation  $C \ll 1$ . The quantity  $C$  is the slope of the sides of the triangle relative to the stream direction and is equal to one-fourth the aspect ratio. The pressure distributions derived on this assumption can be shown to be valid only to the first order in  $C$ . (See reference 4, appendix A.) Thus, terms of order  $C^2$  or  $\frac{A^2}{16}$  will be neglected in comparison with unity wherever they appear in the analysis.

The validity of the analysis depends on the assumption that the disturbance parameters  $\alpha$ ,  $\beta$ ,  $pb/2V$ ,  $qc/2V$ , and  $rb/2V$  are small in comparison with unity. As in ordinary lifting-line wing theory, however, terms in  $\alpha^2$  are of interest. Some such terms arise without approximation in the transformation from principal axes to stability axes, but others of order  $C$  (and hence not negligible) result from retention of terms of order  $C^2$ . For consistency, therefore, it has appeared necessary to neglect all terms of order  $\alpha^2$  in the treatment.

In the determination of certain of the stability derivatives, two cases will be considered. Case 1 is for a configuration having no dihedral and case 2, for a configuration having a small dihedral angle.

DERIVATIVES  $C_{L\alpha}$ ,  $C_{L\dot{\alpha}}$ , AND  $C_{m\dot{\alpha}}$ 

The derivative  $C_{L\alpha}$  is obtained in reference 2. For accelerated motion the local pressure difference therein must be increased by the term

$$\Delta P = 2\rho \frac{\partial \phi}{\partial t}$$

evaluated relative to axes fixed in the airfoil. This is

$$\Delta P = 2\rho \frac{\partial \phi}{\partial \alpha} \dot{\alpha} \quad (2)$$

If the (small) angle of attack is  $\alpha$ , the flow pattern in a plane cutting the airfoil at a distance  $x$  from the nose is the two-dimensional flow caused by a flat plate having the normal velocity  $\alpha V$ . The surface potential is (reference 2)

$$\begin{aligned} \phi &= \frac{1}{2} \alpha V a \sin \eta \\ &= \frac{1}{2} \alpha V \sqrt{a^2 - y^2} \end{aligned} \quad (3)$$

where  $\cos \eta = \frac{y}{a}$  and the sign changes in going from the upper surface to the lower surface of the airfoil. Differentiation of  $\phi$  with respect to  $\alpha$  and substitution in equation (2) yield

$$\Delta P = 2\rho \dot{\alpha} V a \sin \eta$$

Integration over the plan form gives the total incremental lift caused by  $\dot{\alpha}$  as

$$L' = \frac{\pi}{12} \rho V b^2 c \dot{\alpha}$$

This lift divided by  $\frac{1}{2}\rho V^2 S$  is the incremental lift coefficient, and the derivative of this coefficient with respect to  $\dot{\alpha}\bar{c}/2V$  is the stability derivative  $C_{L\dot{\alpha}}$ . It is

$$C_{L\dot{\alpha}} = \frac{\pi A}{2} \quad (4)$$

The center of pressure of the distribution of  $\Delta P$  is found to be at  $x = \frac{3}{4}c$ . The pitching moment about  $x = \frac{2}{3}c$  is therefore

$$\begin{aligned} M &= -\left(\frac{3}{4}c - \frac{2}{3}c\right)L' \\ &= -\frac{\pi}{144}\rho V b^2 c^2 \dot{\alpha} \end{aligned}$$

This moment divided by  $\frac{1}{2}\rho V^2 S \bar{c}$  is the pitching-moment coefficient, and its derivative with respect to  $\dot{\alpha}\bar{c}/2V$  is the stability derivative  $C_{m\dot{\alpha}}$ . It is

$$C_{m\dot{\alpha}} = -\frac{\pi A}{16} \quad (5)$$

#### DERIVATIVES $C_{Lq}$ AND $C_{mq}$

An angular velocity of pitch  $q$  introduces a variation of angle of attack along the x-axis,

$$\alpha = \alpha_0 + \frac{\left(x - \frac{2}{3}c\right)q}{V}$$

where  $\alpha_0$  is the angle of attack at  $x = \frac{2}{3}c$ . This variable  $\alpha$  is to be substituted in equation (3) for the potential,

$$\begin{aligned} \phi &= \alpha V \sqrt{a^2 - y^2} \\ &= \alpha V a \sin \eta \end{aligned}$$

Equation (1) for the pressure difference between the upper and lower surfaces of the airfoil may be written

$$\Delta P = 2\rho V \frac{\partial \phi}{\partial x}$$

Carrying out the indicated differentiation gives

$$\Delta P = 2\rho V \left[ V\alpha_0 + q \left( x - \frac{2}{3}c \right) \right] \csc \eta \frac{da}{dx} + 2\rho V q a \sin \eta$$

The integration of  $\Delta P$  over the area of the triangle gives the value of lift found in reference 2 for an angle of attack  $\alpha_0$ , plus the additional term

$$L' = \frac{\pi}{6} \rho V^2 b^2 \frac{qc}{2V}$$

The coefficient is formed by division by  $\frac{1}{2}\rho V^2 S$ , and its derivative with respect to  $q\bar{c}/2V$  is the stability derivative  $C_{Lq}$ . It is

$$C_{Lq} = \frac{\pi A}{2} \quad (6)$$

The integration of  $\left( \frac{2}{3}c - x \right) \Delta P$  over the area of the triangle yields the pitching moment about the reference point  $\left( \frac{2}{3}c, 0 \right)$ . This moment is

$$M = -\frac{\pi}{24} \rho V^2 b^2 c \frac{qc}{2V}$$

The coefficient is defined as the moment divided by  $\frac{1}{2}\rho V^2 S \bar{c}$  and its derivative with respect to  $q\bar{c}/2V$  is the stability derivative  $C_{mq}$ . The derivative is

$$C_{mq} = -\frac{3\pi A}{16} \quad (7)$$

DERIVATIVE  $C_{lp}$ 

For the airfoil in rolling motion, any section  $x = \text{constant}$  is a rotating straight line. Lamb (reference 5) gives the potential of the two-dimensional flow produced by the rotation of an ellipse about its center. In the limiting case for which the ellipse becomes a straight line, the surface potential is

$$\begin{aligned}\phi &= \frac{1}{4} \rho a^2 \sin 2\eta \\ &= \frac{1}{2} \rho V \sqrt{a^2 - y^2}\end{aligned}\quad (8)$$

where  $p$  is the angular velocity,  $a$  is the semiwidth of the line, and  $\cos \eta = \frac{y}{a}$ .

Equation (1) for the pressure distribution takes the form

$$\begin{aligned}\Delta P &= 2\rho V \frac{d\phi}{dx} \\ &= 2\rho V \frac{d\phi}{da} \frac{da}{dx}\end{aligned}$$

By use of equation (8), with  $C = \frac{da}{dx}$ , this expression becomes

$$\begin{aligned}\Delta P &= \rho V p C^2 x \frac{y/a}{\sqrt{1 - \frac{y^2}{a^2}}} \\ &= \rho V p C^2 x \cot \eta\end{aligned}\quad (9)$$

This antisymmetric pressure distribution due to rolling was first obtained and shown graphically in reference 4. Figures 4 and 5 herein are reproduced from this reference. Figure 4 may be compared with figure 3 of reference 2 which shows the pressure distribution due to angle of attack.

The spanwise loading, following reference 2, is merely

$$\frac{dL'}{dy} = 2\rho V\phi$$

with  $\phi$  evaluated at the trailing edge of the airfoil. The distribution is shown in figure 5.

The integration of  $\frac{dL'}{dy} y$  dy across the span gives the rolling moment

$$L = -\frac{\pi}{128} \rho b^4 V p$$

Division by  $\frac{1}{2}\rho V^2 S b$  converts this moment to coefficient form, and the derivative with respect to  $pb/2V$  is the stability derivative  $C_{l_p}$ . It is

$$\begin{aligned} C_{l_p} &= -\frac{\pi}{32} \frac{b^2}{S} \\ &= -\frac{\pi}{32} A \end{aligned} \quad (10)$$

#### DERIVATIVE $C_{l_\beta}$

##### Case 1, No Dihedral

The pressure difference across a thin airfoil in steady flow has been given by equation (1)

$$\Delta P = 2\rho V u_o$$

where  $u_o$  is the component of induced velocity parallel to the stream direction, measured along the upper surface. If sideslip occurs, the stream direction is inclined relative to the x-axis of

the airfoil by the sideslip angle  $\beta$ . Thus, with  $\beta$  positive for sideslip in the positive direction along the y-axis,

$$u_o = \cos \beta \frac{\partial \phi}{\partial x} - \sin \beta \frac{\partial \phi}{\partial y}$$

$$\approx \frac{\partial \phi}{\partial x} - \beta \frac{\partial \phi}{\partial y}$$

where  $\beta^2 \ll 1$ . Hence,

$$\Delta P = 2\rho V \left( \frac{\partial \phi}{\partial x} - \beta \frac{\partial \phi}{\partial y} \right) \quad (11)$$

The surface potential  $\phi$  for the disturbance velocity depends only on the normal velocity of points of the surface. The potential is therefore unaffected by sideslip when there is no dihedral. In the present case the normal velocity is  $\alpha V$  due to angle of attack and the appropriate potential is that discussed in the section on  $C_{L\alpha}$  and  $C_{m\alpha}$  and given by equation (3). Carrying out the differentiations indicated in equation (11) gives, after simplification,

$$\Delta P = 2\rho V^2 \alpha \left( \frac{da}{dx} \csc \eta + \beta \cot \eta \right) \quad (12)$$

The symmetric first term is the lift distribution in the absence of sideslip. This term yields no rolling moment. The antisymmetric second term contributes the rolling moment

$$L = -\frac{\pi}{12} \rho V^2 b^2 c \alpha \beta$$

The coefficient is formed by division by  $\frac{1}{2} \rho V^2 S b$ , and its derivative with respect to  $\beta$  is the stability derivative  $C_{l\beta}$ . It is

$$(C_{l\beta})_{\alpha} = -\frac{\pi}{3} \alpha \quad (13)$$

Case 2, Dihedral Angle  $\Gamma$ 

If the wing has a small dihedral angle  $\Gamma$  (case 2), the angle of attack on the left panel is reduced in sideslip by the amount  $\beta\Gamma$  and the angle of attack on the right panel is increased by that amount. The flow pattern in a plane cutting the airfoil at a distance  $x$  from the nose can be obtained by a slight modification of the classical thin airfoil theory. (See reference 6.) The left edge and right edge of the section at  $x$  are to be identified, respectively, with the leading edge and trailing edge of the section of thin airfoil theory. The section is regarded as a small deviation from its chord. A distribution of vorticity along the chord of the section is imagined. Paraphrasing Glauert (reference 6), the induced velocity  $w$  is determined for points on the chord but may be taken to be the same for the corresponding points of the section itself. The direction of the resultant velocity adjacent to the airfoil must be parallel to the surface so that at each point of the left panel

$$\frac{w}{V} = -\beta\Gamma + \alpha \quad (14a)$$

and at each point of the right panel

$$\frac{w}{V} = \beta\Gamma + \alpha \quad (14b)$$

The potential corresponding to  $\alpha$  is already known; therefore, only the case for  $\alpha = 0$  need be treated.

The vorticity assumed in the thin airfoil theory (reference 6) has a net circulation to satisfy the Kutta condition at the trailing edge. The addition of a term  $-2V\left(A_0 + \frac{1}{2}A_1\right) \csc \eta$  (with  $\eta$  written for Glauert's  $\theta$ ) eliminates the circulation while retaining certain mathematical properties. With this added term the vorticity is given as

$$k = 2V\left(A_0 \cot \eta - \frac{A_1}{2} \csc \eta + \sum_1^{\infty} A_n \sin n\eta\right) \quad (15)$$

The velocity potential on the upper surface of the section is related to the vorticity  $k$  by

$$\phi = \frac{1}{2} \int_y^a -k \, dy$$

The angle  $\eta$ , originally identified with Glauert's  $\theta$ , is now defined differently so that  $y = a \cos \eta$ . Then the integration of the equation for  $\phi$  with  $dy = -a \sin \eta \, d\eta$  gives

$$\phi = aV \left\{ -A_0 \sin \eta + \frac{A_1}{4} \sin 2\eta + \sum_2^{\infty} \frac{A_n}{2} \left[ \frac{\sin (n+1)\eta}{n+1} - \frac{\sin (n-1)\eta}{n-1} \right] \right\} \quad (16)$$

Equation (16) expresses the upper surface potential for an arbitrary distribution of induced vertical velocity along a line in two-dimensional flow without circulation.

The coefficients in equation (16) are still to be evaluated. The calculation given on pages 88 to 90 of reference 6 when applied to equation (15) leads to

$$\frac{w}{V} = -A_0 + \sum_1^{\infty} A_n \cos n\eta$$

for the ratio of the induced downward velocity to the stream velocity. The coefficients are given by the theory of Fourier series as

$$\left. \begin{aligned} A_0 &= -\frac{1}{\pi} \int_0^{\pi} \frac{w}{V} \, d\eta \\ A_n &= \frac{2}{\pi} \int_0^{\pi} \frac{w}{V} \cos n\eta \, d\eta \end{aligned} \right\} \quad (17)$$

For the sideslipping airfoil section with dihedral angle, the boundary conditions on  $w/V$  has been given in equations (14a) and (14b). By equation (17) the coefficients in this case are, for  $\alpha = 0$ ,

$$\left. \begin{aligned} A_0 &= 0 \\ A_n &= \frac{4\beta\Gamma}{\pi n} \sin \frac{n\pi}{2} \end{aligned} \right\} \quad (18)$$

With the coefficients given in equation (18), then, equation (16) represents the additional potential due to dihedral that may be substituted in equation (11). The term  $\beta \frac{\partial \phi}{\partial y}$  is found to be of the order  $\beta^2$  and thus may be neglected for the present purpose. Integrating the pressure chordwise gives the incremental spanwise load distribution caused by dihedral as

$$\begin{aligned} \frac{dL'}{dy} &= \int_{L.E.}^{T.E.} \Delta P \, dx \\ &= 2\rho V \phi_{T.E.} \end{aligned}$$

The rolling moment is

$$\begin{aligned} L &= - \left( \int_{-a}^a \frac{dL'}{dy} \, dy \right)_{T.E.} \\ &= \left( \rho V a^2 \int_{\pi}^0 \phi \sin 2\eta \, d\eta \right)_{T.E.} \\ &= - \left[ \frac{\pi}{8} \rho V^2 a^3 (A_1 - A_3) \right]_{T.E.} \end{aligned}$$

By equation (18)  $A_1 = \frac{4\beta\Gamma}{\pi}$  and  $A_3 = -\frac{4\beta\Gamma}{3\pi}$ , and at the trailing edge  $a = \frac{b}{2}$ . Thus, for the present case

$$L = -\frac{1}{12}\rho v^2 b^3 \beta \Gamma$$

The coefficient is formed by division by  $\frac{1}{2}\rho v^2 S b$  and its derivative with respect to  $\beta$  is the stability derivative  $C_{L\beta}$  for zero angle of attack. The derivative is

$$(C_{L\beta})_{\Gamma} = -\frac{1}{6}A\Gamma$$

The complete stability derivative is obtained by adding to the preceding equation the contribution of angle of attack given in equation (13) so that

$$C_{L\beta} = -\frac{\pi}{3}\alpha - \frac{A}{6}\Gamma \quad (19)$$

#### DERIVATIVE $C_{Lr}$

##### Case 1, No Dihedral

The reference point for these calculations is at a distance  $\frac{2c}{3}$  from the vertex of the triangle, measured along the x-axis. Let the stream velocity at this point be  $V$ . Then, if the yawing velocity is  $r$ , the longitudinal velocity at  $(x,y)$  is  $V - ry$  and the sideslip velocity is  $-r(x - \frac{2c}{3})$ . Let these expressions replace  $V$  and  $\beta V$ , respectively, in equation (11) so that

$$\Delta P = 2\rho \left[ (V - ry) \frac{\partial \phi}{\partial x} + r \left( x - \frac{2c}{3} \right) \frac{\partial \phi}{\partial y} \right]$$

The appropriate potential  $\phi$  is that given by equation (3), which is

$$\phi = \alpha V a \sin \eta$$

Carrying out the indicated operation gives

$$\Delta P = 2\rho \left[ V^2 \alpha C \csc \eta - r V \alpha \left( x - \frac{2}{3}c + aC \right) \cot \eta \right] \quad (20)$$

where  $C \equiv \frac{da}{dx} \ll 1$ . The term  $aC = xC^2$  and is negligible in comparison with  $x$  to the first order in  $C$ .

The symmetric cosecant term is the lift distribution in straight flight; it yields no rolling moment. The antisymmetric cotangent term contributes the rolling moment

$$L = 2\rho \int_0^c \int_{-a}^a r V \alpha \left( x - \frac{2}{3}c \right) \cot \eta \, y \, dx \, dy$$

With  $\eta = \arccos \frac{y}{a}$ , this moment is evaluated as

$$L = \frac{\pi}{144} \rho V r a b^2 c^2$$

The coefficient is defined as the moment divided by  $\frac{1}{2} \rho V^2 S b$ , and its derivative with respect to  $rb/2V$  is the stability derivative  $C_{l_r}$  for zero dihedral. It is

$$(C_{l_r})_\alpha = \frac{\pi a}{9A} \quad (21)$$

Case 2, Dihedral Angle  $\Gamma$ 

In the section on  $C_{l\beta}$  dihedral was shown to add an additional term, which is given by equation (16), to the potential, where the constants  $A_n$  are given by equation (18). In the present section the variable sideslip angle  $-\frac{r}{V}(x - \frac{2}{3}c)$  replaces the constant sideslip angle  $\beta$  of the section on  $C_{l\beta}$ . The rolling moment due to the additional term is thus

$$L = -\left[\frac{\pi}{8}\rho V^2 a^3 (A_1 - A_3)\right]_{T.E.}$$

as was found in the section on  $C_{l\beta}$ . By equation (18), with  $\beta = -\frac{r}{V}(x - \frac{2}{3}c)$ ,

$$A_1 = -\frac{4\Gamma}{\pi} \frac{r}{V} \left(x - \frac{2}{3}c\right)$$

$$A_3 = \frac{4}{3} \frac{\Gamma}{\pi} \frac{r}{V} \left(x - \frac{2}{3}c\right)$$

The substitution of the values of  $a$ ,  $A_1$ , and  $A_3$  at the trailing edge, where  $a = \frac{b}{2}$  and  $x = c$ , gives

$$L = \frac{1}{36}\rho V r \Gamma b^3 c$$

The coefficient is formed as before by division by  $\frac{1}{2}\rho V^2 S b$ , and its derivative with respect to  $rb/2V$  is

$$(C_{l_r})_{\Gamma} = \frac{2}{9}\Gamma$$

This result must be added to the result for case 1 (no dihedral) to give the total value of the stability derivative, as follows:

$$C_{L_r} = \frac{\pi\alpha}{9A} + \frac{2}{9}\Gamma \quad (22)$$

### DERIVATIVES $C_{Y_p}$ AND $C_{n_p}$

#### Case 1, No Dihedral

The side force and yawing moment relative to body axes are contributed entirely by suction along the leading edge of the wing. This suction may be evaluated by considering the triangular wing to have a small thickness so that the sections  $x = \text{constant}$  are ellipses. The lateral component of the pressure distribution is determined and integrated. This approach is given in detail in reference 4 for the case of rolling at zero angle of attack, and its extension to the case of rolling with a small angle of attack was made in the original determination of  $C_{Y_p}$  and  $C_{n_p}$  in the present analysis. A very much simpler method of evaluating the suction is suggested in reference 7, however, and this method is adopted herein.

Consider a condition for which the induced surface velocity normal to the edge is of the form

$$v_H = \pm \frac{G}{\sqrt{s}} \quad (23)$$

in the immediate neighborhood of the edge, where  $s$  is distance from the edge and  $G$  is a constant. Reference 7 points out that for such a flow there is a suction force per unit length of edge which is

$$F = \pi\rho G^2 \quad (24)$$

in an incompressible fluid. For the narrow triangles discussed in this paper the component of the stream velocity normal to the edges is inherently small compared with the velocity of sound over the range of stream Mach numbers considered. Thus, no compressibility correction is necessary.

For the triangular wing in rolling motion the induced velocity component  $u$  has been obtained as a factor in equation (9) and may be written

$$u_1 = \pm \frac{\frac{1}{2}\rho y c^2}{\sqrt{c^2 - \left(\frac{y}{x}\right)^2}}$$

Angle of attack will give the additional contribution (reference 2)

$$u_2 = \pm \frac{\alpha V c^2}{\sqrt{c^2 - \left(\frac{y}{x}\right)^2}}$$

The total induced velocity component  $u$  on the upper surface is thus

$$u = \frac{c^2 \left( \alpha V + \frac{1}{2} \rho y \right)}{\sqrt{c^2 - \left(\frac{y}{x}\right)^2}}$$

Very near the edge this expression is approximately

$$u = \frac{c^{3/2} \left( \alpha V \pm \frac{1}{2} \rho c x \right)}{2^{1/2} \sqrt{c - \left| \frac{y}{x} \right|}}$$

where the plus sign refers to the right edge and the minus sign to the left edge.

If a similar calculation is made for  $v = \frac{\partial \phi}{\partial y}$ , it is found that as the edge is approached the resultant induced velocity  $\sqrt{u^2 + v^2}$  becomes normal to the edge. Thus, the normal velocity near the edge is

$$v_N = \frac{\sqrt{1 + c^2}}{c} u$$

$$\approx \frac{u}{c}$$

to the first order in  $C$ . The perpendicular distance of point  $(x, y)$  from the edge is, to the same degree of accuracy,

$$s \approx x \left( C - \left| \frac{y}{x} \right| \right)$$

The induced surface velocity very near the edge may therefore be expressed approximately as

$$v_N = \left( \alpha v \pm \frac{1}{2} p C x \right) \sqrt{\frac{C x}{2 s}}$$

which is of the form of equation (23) already considered. The suction force per unit length of edge by equation (24) is thus

$$F = \pi \rho G^2$$

$$= \frac{\pi}{2} \rho C x \left( \alpha^2 v^2 + \frac{1}{4} p^2 C^2 x^2 \pm \alpha v p C x \right)$$

where the plus sign refers to the right edge and the minus sign refers to the left edge.

The lateral component of this suction force is given by

$$Y = \int_0^{c'} (F_R - F_L) dx$$

$$= \frac{\pi}{3} \rho C^2 c^3 \alpha v p$$

The coefficient is formed by division by  $\frac{1}{2}\rho V^2 S$ , and the derivative with respect to  $pb/2V$  is the stability derivative  $C_{Y_p}$ . It is

$$(C_{Y_p})_\alpha = \frac{2}{3}\pi\alpha \quad (25)$$

The moment of the leading-edge suction about the vertex of the triangle is approximately, for  $C^2 \ll 1$ ,

$$\begin{aligned} N_o &= - \int_0^c (F_R - F_U) x \, dx \\ &= - \frac{\pi}{4} \rho C^2 c^4 \alpha V_p \end{aligned}$$

The moment about the reference point  $(\frac{2}{3}c, 0)$  is

$$\begin{aligned} N &= N_o + \frac{2}{3}cY \\ &= - \frac{\pi}{36} \rho C^2 c^4 \alpha V_p \end{aligned}$$

The moment coefficient is formed by division by  $\frac{1}{2}\rho V^2 S b$ , and the derivative with respect to  $pb/2V$  is the stability derivative  $C_{n_p}$ . It is

$$(C_{n_p})_\alpha = - \frac{\pi\alpha}{9A} \quad (26)$$

#### Case 2, Dihedral Angle $\Gamma$

To the first order in the dihedral angle  $\Gamma$ , dihedral will not change the pressure distribution. The inclination of the wing panels, however, will give rise to a lateral force component, as follows:

$$Y = -\Gamma \iint \Delta P \, dx \, dy$$

for the right wing panel, and a similar expression with opposite sign for the left wing panel. The pressure difference  $\Delta P$  has been evaluated in equation (9) of the section on  $C_{L_p}$ . With this value the integration gives

$$Y = -\frac{1}{12} \rho V \Gamma b^3 p$$

Division by  $\frac{1}{2} \rho V^2 S$  and differentiation with respect to  $pb/2V$  give the increment to the stability derivative  $C_{Y_p}$  caused by dihedral as

$$\left( C_{Y_p} \right)_{\Gamma} = -\frac{1}{3} A \Gamma$$

By addition of the value obtained for the case of no dihedral, the complete derivative  $C_{Y_p}$  is

$$C_{Y_p} = \frac{2}{3} \pi \alpha - \frac{A}{3} \Gamma \quad (27)$$

The pressure distribution is such that along any radial line from the vertex the pressure increases in proportion to  $x$ . For such a distribution the center of pressure on each panel is at  $\frac{3}{4}c$  from the vertex. The yawing moment about the reference point  $\left( \frac{2}{3}c, 0 \right)$  is

$$\begin{aligned} N &= -\left( \frac{3}{4}c - \frac{2}{3}c \right) Y \\ &= -\frac{1}{144} \rho V \Gamma b^3 c p \end{aligned}$$

Division by  $\frac{1}{2}\rho V^2 S b$  and differentiation with respect to  $pb/2V$  give the increment to  $C_{n_p}$  caused by dihedral as

$$(C_{n_p})_{\Gamma} = \frac{1}{18}\Gamma$$

By addition of the value obtained for no dihedral the complete derivative is therefore

$$C_{n_p} = -\frac{\pi\alpha}{9A} + \frac{\Gamma}{18} \quad (28)$$

#### DERIVATIVES $C_{Y\beta}$ AND $C_{n\beta}$

##### Case 1, No Dihedral

A little sideslip can readily be shown to have negligible effect on the symmetrical distribution of suction along most of the leading edge. Near the trailing edge some modification may be expected at subsonic speeds due to the altered direction of the trailing vortex sheet. Any lateral force and yawing moment would have to come from the small disturbed region. Examination indicates that such a force or moment would be of order  $\alpha^2\beta$  and hence zero to the first order in  $\alpha$ .

##### Case 2, Dihedral Angle $\Gamma$

The contribution of dihedral to the velocity component  $u$  induced in sideslip is obtained by differentiating equation (16) with respect to  $x$ . A term  $\alpha VC \csc \eta$  must be added for the effect of angle of attack. After insertion of the constants from equation (18) the total velocity component  $u$  is obtained as

$$u = \alpha VC \csc \eta + \frac{2}{\pi} \Gamma CV \left\{ \frac{\sin 2\eta}{2} + \cos 2\eta \cot \eta - \sum_3^{\infty} \sin \frac{n\pi}{2} \left[ \frac{\sin (n+1)\eta}{n+1} + \frac{\sin (n-1)\eta}{n-1} \right] \right\} \quad (29)$$

The only terms that approach infinity near the edges (that is, as  $\eta \rightarrow 0$  or  $\pi$ ) are the cosecant term and the cotangent term. In that region both terms behave like  $\sqrt{\frac{Cx}{2s}}$ , with appropriate sign, where  $s$  is the perpendicular distance from the edge. The velocity component  $u$  there may thus be written

$$u = \left( \alpha \pm \frac{2}{\pi} \beta \Gamma \right) v \sqrt{\frac{Cx}{2s}}$$

where the plus sign refers to the right edge and the minus sign to the left edge.

If a similar calculation is made for  $v = \frac{\partial b}{\partial y}$ , it is found as before that near the edge the normal induced velocity  $v_N$  is approximately equal to  $u/C$  to the first order in  $C$ . Thus,  $v_N$  is of the form  $\frac{G}{\sqrt{s}}$ , and the corresponding suction force per unit length edge is  $F = \pi \rho G^2$ , as indicated in a preceding section. Substitution of the expression for  $G$ , neglect of terms of the second order in  $\beta$ , and simplification gives

$$F = \frac{\pi}{2} \rho v^2 C x \left( \alpha^2 \pm \frac{4}{\pi} \alpha \beta \Gamma \right) \quad (30)$$

The lateral component of this suction force is

$$\begin{aligned} Y_1 &\approx \int_0^c (F_R - F_L) dx \\ &= 2 \rho v^2 C c^2 \alpha \beta \Gamma \end{aligned} \quad (31)$$

There is an additional lateral force due to a component of the pressure acting on the inclined panels. The part of the pressure caused by dihedral will contribute terms of order  $\Gamma^2$ . To the first order in  $\Gamma$ , then, only the pressure distribution

in the absence of dihedral (equation (12)) need be considered. Further, only the antisymmetric cotangent term will contribute to the lateral force. The incremental lateral force is thus

$$\begin{aligned}
 Y_2 &= -2\Gamma \iint 4\alpha \frac{1}{2}\rho V^2 \beta \cot \eta \, dy \, dx \\
 &= -4\rho V^2 \alpha \beta \Gamma \int_0^c \int_0^{\pi/2} C_x \cos \eta \, d\eta \, dx \\
 &= -2\rho V^2 c c^2 \alpha \beta \Gamma \quad (32)
 \end{aligned}$$

The total lateral force to the first order in  $\Gamma$  is  $Y_1 + Y_2$ . This sum is seen to be zero, and hence the lateral force derivative  $C_{Y\beta}$  is likewise zero.

Equation (12) shows that sideslip gives rise to a pressure distribution that is constant along radial lines from the vertex of the triangle. (Such a pressure distribution defines a conical flow field.) Equation (12) is for zero dihedral, but equation (16) leads to the same behavior for the triangle with dihedral. The center of pressure on each panel of the triangle will be on the line  $x = \frac{2}{3}c$ . So also will the center of pressure of the leading-edge suction. There is thus no yawing moment about the reference point  $(\frac{2}{3}c, 0)$ , and the stability derivative  $C_{n\beta}$  is zero.

#### DERIVATIVES $C_{Yr}$ AND $C_{nr}$

In the case of yawing motion the local sideslip velocity is  $r(\frac{2}{3}c - x)$ . The suction  $F$  per unit length of the leading edge is obtained by substituting this local sideslip velocity for  $\beta V$  in equation (30) derived for sideslip, as follows:

$$F = \frac{\pi}{2} \rho V^2 C_x \left[ \alpha^2 \pm \frac{4}{\pi} \frac{\alpha \Gamma}{V} \left( \frac{2}{3} c - x \right) \right]$$

(When  $\beta$  varies with  $x$ , as in the present case, equation (29) requires an additional term in  $\frac{d\beta}{dx}$ , proportional to  $\Gamma$ . This term is finite at the edges and, therefore, does not contribute to the expression for  $Y$ .)

The lateral component of this suction force is

$$\begin{aligned} Y_1 &= \int_0^c (F_R - F_L) dx \\ &= 0 \end{aligned} \quad (33)$$

The antisymmetric cotangent part of the pressure distribution in equation (20) may contribute a lateral force because of the inclination of the panels. To the first order in  $\Gamma$ , this is the only contribution, according to the reasoning in the section on  $C_{Y\beta}$  and  $C_{n\beta}$ . The contribution is, to the first order in  $C$ ,

$$\begin{aligned} Y &= 4\rho V \alpha \Gamma \int_0^c \int_0^a \left( x - \frac{2}{3}c \right) \cot \eta \, dy \, dx \\ &= 4\rho V \alpha \Gamma \int_0^c \int_0^{\pi/2} \left( x - \frac{2}{3}c \right) Cx \cos \eta \, d\eta \, dx \\ &= 0 \end{aligned} \quad (34)$$

The total lateral force caused by yawing motion is  $Y_1 + Y_2$ . The lateral force derivative  $C_{Yr}$  is accordingly zero.

The leading-edge suction gives rise to a pure yawing couple. This couple is conveniently obtained by computing the moment of the suction force about the vertex of the triangle, as follows ( $C^2 \ll 1$ ):

$$\begin{aligned}
 N_1 &\approx - \int_0^c (F_R - F_L) x \, dx \\
 &= \frac{1}{9} \rho V^2 \alpha r^2 C_c^4 \quad (35)
 \end{aligned}$$

The pressure distribution on the inclined panels of the wing will have a lateral component that likewise contributes a pure yawing couple. From equation (20) the couple is, to the first order in  $C$ ,

$$\begin{aligned}
 N_2 &\approx -4\Gamma\rho V\alpha \int_0^c \int_0^a \left(x - \frac{2c}{3}\right) \cot \eta \, x \, dy \, dx \\
 &= -4\Gamma\rho V\alpha C \int_0^c \int_0^{\pi/2} \left(x - \frac{2c}{3}\right) x^2 \cos \eta \, d\eta \, dx \\
 &= -\frac{1}{9} \rho V \alpha r^2 C_c^4 \quad (36)
 \end{aligned}$$

A third yawing couple will be contributed by skin friction. (Skin friction has not been considered in evaluating the other stability derivatives because its direct contribution is expected to be unimportant. The indirect effect of skin friction in influencing the pressure distribution via the boundary layer may indeed be important, although it is not treated.)

The skin friction couple is approximately given by:

$$N_3 = \int_0^c \int_{-a}^a C_{D_0} \frac{1}{2} \rho V_R^2 \left[ \left(x - \frac{2c}{3}\right) \beta + y \right] dx \, dy$$

where  $V_R$  is the resultant velocity and  $V_R^2 = (V - ry)^2 + r^2 \left(x - \frac{2c}{3}\right)^2$ ,

$\beta$  is the local sideslip angle and equals  $\frac{-r \left(x - \frac{2c}{3}\right)}{V}$ , and  $C_{D_0}$  is the section drag coefficient which is taken equal to wing profile drag coefficient.

To the first order in  $r$  this expression is

$$N_3 = -\frac{1}{2}\rho C_{D0} \int_0^c \int_{-a}^a \left\{ Vr \left[ \left( x - \frac{2}{3}c \right)^2 + 2y^2 \right] - v^2 y \right\} dx dy$$

$$= -\frac{1}{36}\rho Vr C_{D0} Cc^4 (1 + 6C^2)$$

The total yawing moment caused by yawing motion is  $N_1 + N_2 + N_3$ , which is just  $N_3$  because  $N_1$  and  $N_2$  cancel. The coefficient is  $N_3$  divided by  $\frac{1}{2}\rho V^2 S b$  and the derivative with respect to  $\frac{rb}{2V}$  is the stability derivative  $C_{n_r}$ . Carrying out these operations gives

$$C_{n_r} = -\left( \frac{1}{6} + \frac{4}{9A^2} \right) C_{D0} \quad (37)$$

A similar calculation shows that the side force due to skin friction is zero.

## RESULTS AND DISCUSSION

The values obtained for the stability derivatives are summarized in table I with respect to two systems of axes. One system is the principal body axes of figure 1 with origin at the aerodynamic center  $\left( \frac{2}{3}c, 0, 0 \right)$ . The other system is the stability axes shown in figure 3 with origin a distance  $x_{cg}$  ahead of the  $\frac{2}{3}c$  point.

These stability derivatives apply to an isolated triangular wing in the limiting case of aspect ratio approaching zero. Applicability decreases with increasing aspect ratio, and an aspect ratio 0.5 is estimated as the upper limit of utility. The mathematical validity at the very low aspect ratios may be offset, perhaps, by error due to the neglected boundary layer.

The arguments for the effects of compressibility presented in reference 2 can be carried over to the present work. The stability derivatives presented herein, therefore, are expected to apply at both subsonic and supersonic speeds, with the exception of the transonic region, up to a limiting speed at which the triangle is no longer narrow compared with the Mach cone from its vertex.

The over-all pitching-moment derivatives should be little affected by the addition of a fuselage, the nose of which does not project much beyond the vertex of the triangular wing. The wing will orient the flow along the axis of the fuselage and thereby will eliminate much of the unstable pitching moment of the fuselage. The flow will continue to be essentially axial along the part of the fuselage behind the wing because the low aspect ratio yields a downwash angle substantially equal to the angle of attack.

Theoretical considerations suggest that the unstable yawing moment of the fuselage will add to the value of  $C_{n\beta}$  for the wing alone. Little effect on  $C_{n\beta}$  or  $C_{nr}$  is expected. Little effect on the rolling-moment derivatives is expected if the wing is mounted centrally on the fuselage. High-wing or low-wing arrangements, however, should have pronounced effects on the effective dihedral. These conclusions are only tentative, and a proper evaluation of the wing-fuselage interference must be the subject of further investigation.

Langley Memorial Aeronautical Laboratory  
National Advisory Committee for Aeronautics  
Langley Field, Va., July 15, 1947

## R E F E R E N C E S

1. Munk, Max M.: The Aerodynamic Forces on Airship Hulls. NACA Rep. No. 184, 1923.
2. Jones, Robert T.: Properties of Low-Aspect-Ratio Pointed Wings at Speeds below and above the Speed of Sound. NACA TN No. 1032, 1946.
3. Glauert, H.: A Non-Dimensional Form of the Stability Equations of an Aeroplane. R. & M. No. 1093, British A.R.C., 1927.
4. Ribner, Herbert S.: A Transonic Propeller of Triangular Plan Form. NACA TN No. 1303, 1947.
5. Lamb, Horace: Hydrodynamics. Reprint of sixth ed. (first American ed.), Dover Publications (New York), 1945, pp. 86-88.
6. Glauert, H.: The Elements of Aerofoil and Airscrew Theory. Cambridge Univ. Press, reprint of 1937, pp. 87-90.
7. Brown, Clinton E.: Theoretical Lift and Drag of Thin Triangular Wings at Supersonic Speeds. NACA TN No. 1183, 1946.

TABLE I

STABILITY DERIVATIVES OF LOW-ASPECT-RATIO TRIANGLE

TO FIRST ORDER  $A$ ,  $\alpha$ , AND  $\Gamma$

Stability derivatives	Principal axes (Origin at $\frac{2}{3}c$ from vertex)	Stability axes (Origin at distance $x_{CG}$ ahead of $\frac{2}{3}c$ )
$C_{L\alpha}$	$\frac{\pi}{2}A$	$\frac{\pi}{2}A$
$C_{L\dot{\alpha}}$	$\frac{\pi}{2}A$	$\frac{\pi}{2}A$
$C_{Lq}$	$\frac{\pi}{2}A$	$\frac{\pi}{2}A + \pi A \frac{x_{CG}}{c}$
$C_{m\alpha}$	0	<del><math>-\frac{\pi}{4} \frac{x_{CG}}{c}</math></del> $-\frac{1}{2} \pi A \frac{x_{CG}}{c}$ <i>see erratum</i>
$C_{m\dot{\alpha}}$	$-\frac{\pi}{16}A$	$-\frac{\pi}{16}A - \frac{\pi}{2} \frac{x_{CG}}{c}$
$C_{mq}$	$-\frac{3\pi}{16}A$	$-\frac{3}{16} \pi A - \frac{\pi}{2} \frac{x_{CG}}{c} - \pi A \frac{x_{CG}^2}{8c^2}$
$C_{Y\beta}$	$-\frac{\pi}{3}\alpha - \frac{A}{6}\Gamma$	$\frac{\pi}{3}\alpha - \frac{A}{6}\Gamma$
$C_{Yp}$	$-\frac{\pi}{32}A$	$-\frac{\pi}{32}A + \left(\frac{5}{18} + \frac{8}{9} \frac{x_{CG}}{c}\right) \Gamma \alpha$
$C_{Yr}$	$\frac{\pi\alpha}{9A} + \frac{2}{9}\Gamma$	$\left(\frac{\pi\alpha}{9A} + \frac{\Gamma}{18}\right) \left(1 + \frac{8}{9} \frac{x_{CG}}{c}\right) + \frac{\Gamma}{6}$
$C_{n\beta}$	0	$\frac{A}{6} \Gamma \alpha$
$C_{nr}$	$-\frac{\pi\alpha}{9A} + \frac{\Gamma}{18}$	$\left(-\frac{\pi\alpha}{9A} + \frac{\Gamma}{18}\right) \left(1 + \frac{8}{9} \frac{x_{CG}}{c}\right)$
$C_{nr}$	$-\left(\frac{1}{6} + \frac{4}{9A^2}\right) C_{D0}$	$-\left(\frac{1}{6} + \frac{4}{9A^2}\right) C_{D0} - \left(\frac{5}{18} + \frac{8}{9} \frac{x_{CG}}{c}\right) \Gamma \alpha$
$C_{Y\beta}$	0	0
$C_{Yp}$	$\frac{2}{3}\pi\alpha - \frac{A}{3}\Gamma$	$\frac{2}{3}\pi\alpha - \frac{A}{3}\Gamma$
$C_{Yr}$	0	$\frac{A}{3} \Gamma \alpha$

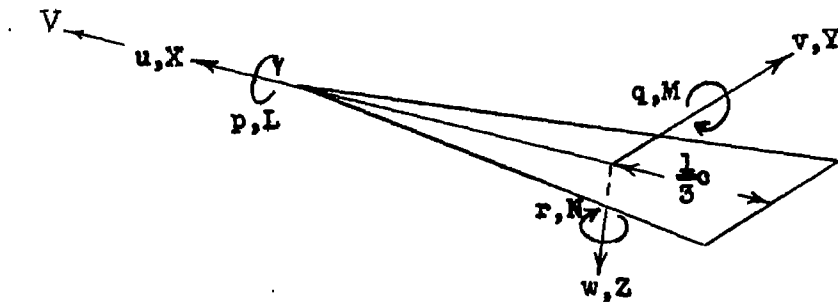


Figure 1.- Velocities, forces, and moments relative to principal axes with origin at  $\frac{2}{3}c$ .

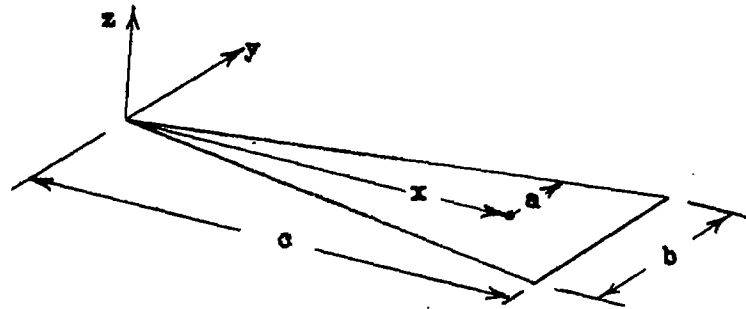


Figure 2.- Axes and notation used in analysis.

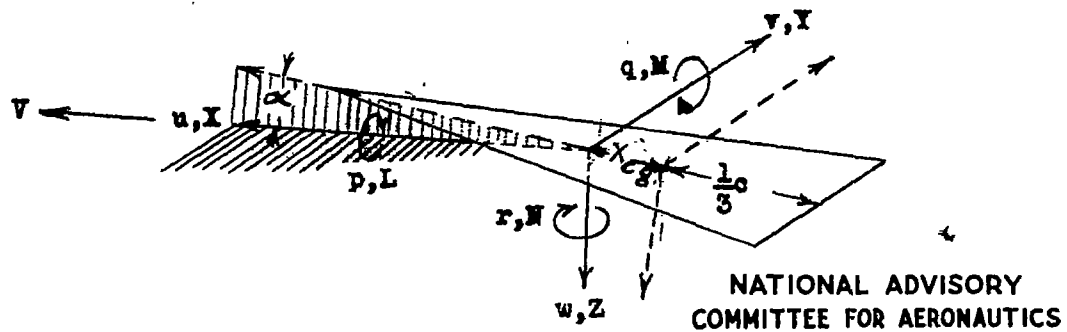


Figure 3.- Velocities, forces, and moments relative to stability axes with origin at  $\frac{2}{3}c - x_{cg}$ . Principal axes of figure 1 dotted in for comparison.

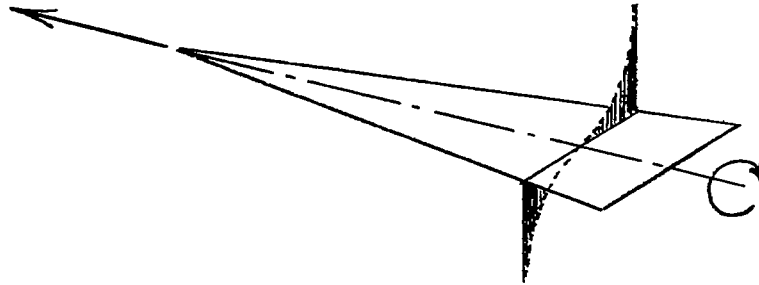


Figure 4.- Distribution of pressure difference caused by rolling.

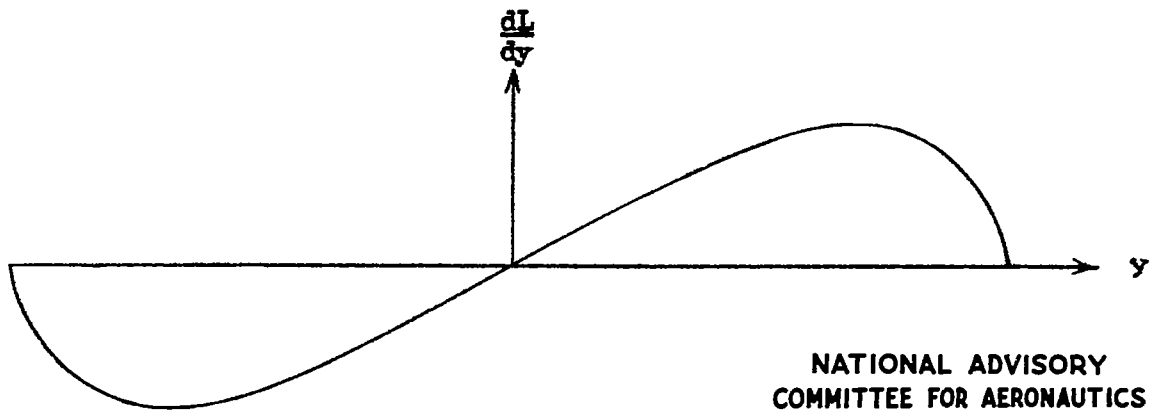


Figure 5.- Distribution along span of normal force caused by rolling.